SPACECRAFT FORMATION CONTROL USING ANALYTICAL INTEGRATION OF GAUSS' VARIATIONAL EQUATIONS

Mohamed Khalil Ben Larbi, Enrico Stoll

Institute of Space Systems
Technische Universitaet Braunschweig
Hermann-Blenk-Str. 23, 38108 Braunschweig, Germany

ABSTRACT

This paper derives a control concept for far range Formation Flight (FF) applications assuming circular reference orbits. The paper focuses on a general impulsive control concept for FF which is then extended to the more realistic case of non-impulsive thrust maneuvers. The control concept uses a description of the FF in relative orbital elements (ROE) instead of the classical Cartesian description since the ROE provide a direct access to key aspects of the relative motion and are particularly suitable for relative orbit control purposes and collision avoidance analysis. Although Gauss' variational equations have been first derived to offer a mathematical tool for processing orbit perturbations, they are suitable for several different applications. If the perturbation acceleration is due to a control thrust, Gauss' variational equations show the effect of such a control thrust on the keplerian orbital elements. Integrating the Gauss' variational equations offers a direct relation between velocity increments in the local vertical local horizontal (LVLH) frame and the subsequent change of keplerian orbital elements. For proximity operations, these equations can be generalized from describing the motion of single spacecraft to the description of the relative motion of two spacecraft. This will be shown for impulsive and finite-duration maneuvers. Based on that, an analytical tool to estimate the error induced through impulsive planning is presented. The resulting control schemes are simple and effective and thus, also suitable for on-board implementation. Simulations show that the proposed concept improves the timing of the thrust maneuver executions and thus reduces the residual error of the formation control.

Index Terms— Gauss' variational equations, relative orbital elements, impulsive thrust, continuous thrust

1. INTRODUCTION

The theory of spacecraft (s/c) formation flying has become the focus of considerably extensive research and development effort during the last decades. Earlier design techniques addressed rendezvous and docking missions such as those of the Apollo space program, which had the Lunar Excursion Module and the Command and Service Module being assembled in orbit. The purpose is not to correct the Earth relative orbit itself during this maneuver, but rather to adjust and control the relative orbit between two vehicles. The relative distance is decreased to zero in a very slow and controlled manner during the docking maneuver [1].

The modern-day focus of s/c formation flying has extended to maintain a formation of various s/c. Several formation flying missions are currently operating or in the deisgn stage: synthetic aperture interferometers for Earth observation (e.g. TanDEM-X/TerraSAR-X), dual s/c telescopes (e.g. XEUS) and laser interferometer for the detection of gravitational waves (e.g. LISA). It became obvious that the formation flying concept overcomes significant technical challenges and even avoids financial limitations. Indeed, the distribution of sensors and payloads among several s/c allows higher redundancy, flexibility, and new applications that would not be achievable with a single s/c [2]. Recently, formation flying with non-cooperative objects has emerged as a new focus, motivated through the increasing number of such objects especially in low Earth Orbit. The exploitation of satellite-based resources has led to an ever increasing number of non-cooperative objects such as defunct satellites and rocket upper stages termed as *space debris*. A collisional cascading effect has been postulated by Kessler in the late seventies [3] and seems more real than ever since 2009 when two intact artificial satellites, Iridium 33 (operational) and Kosmos 2251 (out of service) collided distributing debris across thousands of cubic kilometers. Using the the NASA long-term orbital debris projection model (LEGEND), Liou showed that, besides already implemented mitigation measures, the annual active debris removal (ADR) of 5-10 prioritized objects from orbit, is required in order to stabilize the LEO environment [4]. Those results have been backed by several other studies [5] and meanwhile are widely accepted in the space debris community.

This evolution has led to a substantial research effort to develop a theory that could simply and explicitly address the relative motion and collision avoidance issue in control design. Thus the development of the upcoming theories, such as the relative orbital elements (ROE) and Eccentricity/Inclination (E/I) vector separation, originally developed for collocation of geostationary satellites [6], were conducted.

The control of satellite formation is performed by the activation of on-board thrusters. Typically, impulsive control (very short duration thrust) is preferred to continuous control (finite-duration thrust). This is due to historical limitation on propulsion technologies, typical payload requirements especially for scientific missions, and the simplicity of impulsive planning often allowing pure analytical maneuver design. Recent advances in propulsion and computer technologies suggest a deeper study of continuous planning. This approach is not only justified by the precision of continuous maneuvers planning (the finite duration is explicitly addressed and no impulsive assumptions are made) but also because of the typical advantages of low thrust propulsion systems, such as reduced mass, limited required power, and variable exhaust velocity.

A vast amount of literature exists on formation reconfiguration maneuvers with impulsive thrust mainly modeled with Clohessy-Wiltshire and Lawden's equations of relative motion. The Gauss' variational equations (GVE) of motion however offer an ideal mathematical framework for designing impulsive control laws [7]. These equations have been extensively used in the last decades for absolute orbit keeping of single s/c, but have only recently been exploited for formation flying control in LEO as introduced by Schaub et. al [8] and subsequently by Vaddi et al. [9], Breger et al. [10] and D'amico [11]. The reason for such slow development is that GVE describe the effect of control acceleration on the time derivative of the Keplerian orbital elements which were normally used to parametrize the motion of a single s/c but not the relative motion of a formation [10].

In this paper, we build upon the previously mentioned references and give the following original contributions. Firstly, a comprehensive literature survey of the relative motion parametrization and Gauss' variational equations for relative motion is presented demonstrating the convenience of ROE and GVE-based maneuver planning as opposed to Cartesian parametrization. Secondly, Gauss' variational equation for relative motion using finite duration thrust are derived for a specific set of ROE. Thirdly, an impulsive maneuver plan based on[2] is extended to the general case of non-zero relative semi major axis and finally translated to the case of finite-duration thrust. The paper is organized as follows. In section 2, an overview of the theory of relative motion, including ROE, is presented. In section 3, an overview of the GVE and their application in relative orbit control is presented and the integrated GVE are derived. Section 4 is dedicated to the study of the effects of impulsive and finite duration thrust on ROE. Subsequently the impulsive and finite duration maneuver schemes are derived in section 5 and verified via numerical simulation.

2. DYNAMICS OF RELATIVE MOTION

First of all we define some notations adopted in this paper. The motion of a single s/c orbiting the Earth is described in the Earth Centered Inertial (ECI) frame. The relative motion of two s/c orbiting the Earth is described in the radial-tangential-normal (RTN) frame (Fig. 1).

The $\Delta(.)$ operator indicates arithmetic differences between absolute Cartesian or Orbital parameters. The $\delta(.)$ operator indicates the relative Cartesian position and velocity in the RTN Frame. It refers generally to a non-linear combination of the absolute Cartesian/orbital parameters.

The s/c about which all other s/c motions are referenced is called the *Client* and is denoted with subscript $(\bullet_1)$. The second s/c, referred to as *Servicer*, is to fly in formation with the *Client* and is denoted with the subscript $(\bullet_2)$. Absolute Cartesian and orbital parameters without subscript are to be understood as *Client* parameters.

2.1. Linearized Equations of Relative Motion

The *Client* position vector in the Earth-centered inertial frame (ECI) is noted $\underline{r}_1$. The relative orbit will be described in the rotating local orbital frame RTN in terms of the Cartesian coordinate vector $\delta r = \begin{pmatrix} x & y & z \end{pmatrix}^{\mathrm{T}}$. We introduce dimension-

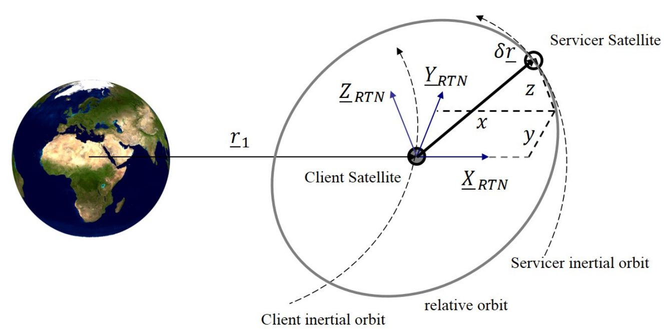

Fig. 1. Illustration of a s/c formation in RTN frame

less spatial coordinates and a dimensionless time τ via the equations:

$$\delta\underline{\rho} = \frac{\delta\underline{r}}{r_1} = \begin{pmatrix} \bar{x} & \bar{y} & \bar{z} \end{pmatrix}^{\mathrm{T}} \text{ and } \mathrm{d}\tau = n\mathrm{d}t \, , \tag{1}$$

$$\delta\underline{\rho} = \frac{\delta\underline{r}}{r_1} = \begin{pmatrix} \bar{x} & \bar{y} & \bar{z} \end{pmatrix}^{\mathrm{T}} \tag{2a}$$

$$\mathrm{d}\tau = n\mathrm{d}t \, , \tag{2b}$$

with n the mean motion. The differentiation with respect to the independent variable τ is written here as

$$()' \equiv \frac{\mathrm{d}\,()}{\mathrm{d}\tau} \ . \tag{3}$$

The dimensionless state vector is then noted

$$\delta \underline{x} = \begin{pmatrix} \delta \underline{\rho} & \delta \underline{\rho}\,' \end{pmatrix}^{\mathrm{T}} \quad . \tag{4}$$

The Clohessy-Wiltshire (CW) equations of motion take a very elegant numerically advantageous form if written in a non-dimensional form [12]:

$$\bar{x}'' - 2\bar{y}' - 3\bar{x} = 0 \tag{5a}$$
$$\bar{y}'' + 2\bar{x}' = 0 \tag{5b}$$
$$\bar{z}'' + \bar{z} = 0 \ . \tag{5c}$$

Note that these equations of motion are valid only if :

- the *Client* orbit is circular,
- $\|\delta\underline{\rho}\| \ll r_1$,
- the *Client* and *Servicer* s/c have a pure Keplerian motion.

Further, the out-of-plane component $\bar{z}$ in equation (5c) decouples from the radial and along track directions (in-plane). A more detailed view on how the equations are obtained can be found in [1, 12].

2.2. Solution of the Linearized Equations of Motion

The CW equations (5) are a set of three coupled ordinary homogeneous second order equations with constant coefficients. Six independent constants are thus required to determine a unique solution for a relative orbit. The general homogenous solution can be written as the product of a state transition matrix $\underline{\underline{\Phi}}(\tau.\tau_0)$ with an integration constants vector $\underline{c}\begin{pmatrix} c_1 & \cdots & c_6 \end{pmatrix}^{\mathrm{T}}$. A possible representation is:

$$\delta\underline{x}(\tau) = \underline{\underline{\Phi}}(\tau,\tau_0)\,\underline{c} \ , \quad \text{with} \quad \underline{\underline{\Phi}}(\tau,\tau_0) =$$

$$\begin{bmatrix} 1 & 0 & -\cos\tau & -\sin\tau & 0 & 0 \\ -\frac{3}{2}(\tau-\tau_0) & 1 & 2\sin\tau & -2\cos\tau & 0 & 0 \\ 0 & 0 & 0 & 0 & \sin\tau & -\cos\tau \\ 0 & 0 & \sin\tau & -\cos\tau & 0 & 0 \\ -\frac{3}{2} & 0 & 2\cos\tau & 2\sin\tau & 0 & 0 \\ 0 & 0 & 0 & 0 & \cos\tau & \sin\tau \end{bmatrix} , \tag{6}$$

and $\underline{c}$ a vector containing a set of six independent integration constants as described in [13]. To study the geometry of the relative path we rewrite the first three rows of equation (6) in amplitude-phase form

$$\bar{x} = \qquad c_1 - c_{34}\cos(\tau-\varphi) \tag{7a}$$
$$\bar{y} = \quad c_2 - c_1\frac{3}{2}(\tau-\tau_0) + 2c_{34}\sin(\tau-\varphi) \tag{7b}$$
$$\bar{z} = \qquad + c_{56}\sin(\tau-\theta) \quad . \tag{7c}$$

The amplitudes and phases of the in-plane and out-of-plane relative motion oscillations are

$$c_{34} = \sqrt{c_3^2 + c_4^2} \qquad c_{56} = \sqrt{c_5^2 + c_6^2} \tag{8}$$
$$\varphi = \arctan\left(\frac{c_4}{c_3}\right) \qquad \theta = \arctan\left(\frac{c_6}{c_5}\right) \ . \tag{9}$$

We can easily see from (7) that the *Servicer* moves in an elliptical-like pattern around the *Client* as illustrated in Fig. 1 and Fig. 2. Indeed:

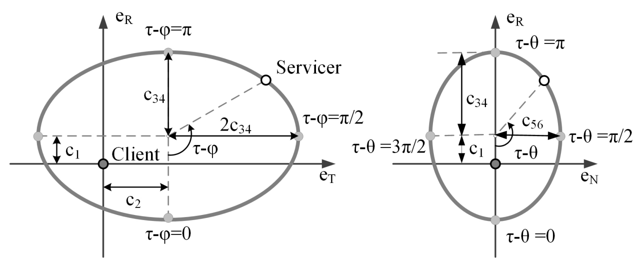

Fig. 2. Illustration of the integration constants in the projected instantaneous (no drift) relative motion ellipse at $\tau = \tau_0$.

- The projection of the relative path in the RT plane is an ellipse centered in (c_1, c_2). Because of the drift term $c_1\frac{3}{2}(\tau-\tau_0)$ the ellipse is instantaneous and the $\bar{y}$-value of the center is valid only at $\tau = 0$. Bounded relative motion is hence obtained for $c_1 = 4\bar{x}_0 + 2\bar{y}_0' = 0$.
- The RN projection is an ellipse centered in $(c_1, 0)$ for $(\varphi-\theta) \in \{0,\pi\}$ which gets tighter and dwindle to a line for $(\varphi-\theta) \to \frac{\pi}{2}$. In the case of bounded relative motion ($c_1 = 0$) the *Client* lies on this line which leads to collision risk if along-track position uncertainties exist and suggests choosing $(\varphi-\theta) \in \{0,\pi\}$ to minimize this risk. This Presumption will be discussed in section 2.4.

2.3. Relative Orbital Elements

In conventional analysis, the set of independent variables $\underline{c}$ could be computed using the initial conditions consisting of the position $\underline{r}$ and velocity $\underline{v}$ at some specific initial time t_0, often taken at zero for convenience. However, any six independent constants can describe the solution, with the physical nature of the problem usually dictating the choice. Many authors worked on that issue searching combinations of Keplerian elements of the co-orbiting s/c to describe their relative motion ([14]). The motivation for this effort was the advantages of the Keplerian elements description, experienced for *single* s/c in the last decades, compared with the classical position-velocity description. Similar advantages were expected and could be noticed. This new approach provides direct insight into the formation geometry and allows the straightforward adoption of variational equations such as the Gauss' ones to study the effects of orbital perturbations on the relative motion.

In this paper a set of non-singular orbital elements $\underline{\alpha} = \begin{pmatrix} a & u & e_x & e_y & i & \Omega \end{pmatrix}^{\mathrm{T}}$ is used to describe the absolute orbit of a s/c with $u = M + \omega$, $e_x = e\cos\omega$, and $e_y = e\sin\omega$ where a denotes the semi major axis, e the eccentricity, i the inclination, Ω the right ascension of the ascending node, ω the argument of periapsis, M the mean anomaly, and u the mean argument of latitude.

We define the ROE introduced by D'Amico [11]:

$$\delta\underline{\alpha} = \begin{pmatrix} \delta a \\ \delta\lambda \\ \delta e_x \\ \delta e_y \\ \delta i_x \\ \delta i_y \end{pmatrix} = \begin{pmatrix} (a_2 - a_1)\, a_1^{-1} \\ (u_2 - u_1) + (\Omega_2 - \Omega_1)\cos i_1 \\ e_{x_2} - e_{x_1} \\ e_{y_2} - e_{y_1} \\ i_2 - i_1 \\ (\Omega_2 - \Omega_1)\sin i_1 \end{pmatrix}, \tag{10}$$

where $\delta\lambda$ denotes the relative mean longitude, $\delta\underline{e}$ and $\delta\underline{i}$ the relative eccentricity and inclination vectors. The ROE defined in (10) are all invariants of the unperturbed relative motion with the exception of $\delta\lambda$, which evolves linearly with time. $\delta\dot{\lambda}$ can be approximated to first order as

$$\delta\dot{\lambda} = \Delta\dot{u} = n_2 - n_1 = -\frac{3}{2} n_1 \frac{\Delta a}{a_1} \tag{11}$$

The general linearized relative motion of the *Servicer* relative to the *Client* is provided in terms of ROE by

$$\delta\alpha_j(t) = \delta\alpha_{j_0} - \frac{3}{2}\left(u(t) - u_0\right)\delta\alpha_{1_0}\ \delta_j^2 \tag{12}$$

where j denotes the vector index ($j = 1, ..., 6$), the subscript 0 indicates quantities at the initial time t_0 and δ_j^2 is the Kronecker delta. Note that the only assumptions made here are pure Keplerian motion and $\Delta u, \Delta a << r_1$. These equations are hence valid for arbitrary eccentricities.

2.4. Final Comments

These ROE have the distinct advantage of matching exactly the integration constants of equation (6) [11]. It follows

$$(c_1, c_2, c_{34}, c_{56}) = (\delta a, \delta\lambda, \|\delta\underline{e}\|, \|\delta\underline{i}\|) \tag{13}$$

φ and θ are the arguments of the vectors $\delta\underline{e}$ and $\delta\underline{i}$ in polar coordinates as depicted in Fig. 3.

That means that the vector $\underline{c}$ is not only an integration constant vector which could be geometrically interpreted in the relative trajectory (Fig. 2) but also receives a geometrical meaning by means of *Servicer*'s and *Client*'s Keplerian elements. Statements about the relative orbit geometry can directly be made based on the absolute Keplerian elements without solving any equation. For example if Δi and $\Delta\Omega$

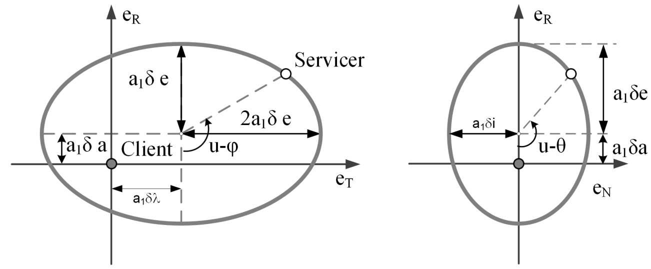

Fig. 3. Illustration of the relative orbital elements in the projected instantaneous (no drift) relative motion ellipse at $u = u_0$.

are found to be zero, then it can immediately be concluded that the amplitude of the out-of-plane motion is zero ($c_{56} = \|\delta\underline{i}\| = \sqrt{(\Delta i)^2 + (\Delta\Omega\sin i_1)^2}$).

Furthermore, we obtain a mapping tool between the relative state vector $\delta\underline{x}(\tau)$ at a generic time τ and the initial ROE vector $\delta\underline{\alpha}(\tau_0)$. Keeping in mind the equivalence between mean argument of latitude u and the independent variable τ, we write :

$$\delta\underline{x}(u) = \underline{\underline{\Phi}}(u, u_0)\delta\underline{\alpha}(u_0) \tag{14}$$

Of practical use is mainly the inverse linear mapping from the relative state vector to the initial ROE vector with $\underline{\underline{\Phi}}^{-1}(u, u_0) =$

$$\begin{bmatrix} 4 & 0 & 0 & 0 & 2 & 0 \\ 6(u-u_0) & 1 & 0 & -2 & 3(u-u_0) & 0 \\ 3\cos u & 0 & 0 & \sin u & 2\cos u & 0 \\ 3\sin u & 0 & 0 & -\cos u & 2\sin u & 0 \\ 0 & 0 & \sin u & 0 & 0 & \cos u \\ 0 & 0 & -\cos u & 0 & 0 & \sin u \end{bmatrix} \tag{15}$$

It may be noted that this choice of the ROE maintain the decoupling of the motion. In other words δa, $\delta\lambda$, and $\delta\underline{e}$ describe the in-plane motion $\delta\underline{i}$ describes the out-of-plane motion.

Moreover the usage of ROE increases the accuracy of the CW general solution because it retains higher order terms which are normally dropped using Cartesian description [1]. For example the first order Cartesian constraint for bounded relative motion ($c_1 = 4\bar{x}_0 + 2\bar{y}_0' = 0$) translated in ROE yields $\delta a = 0$. This is in fact the only condition on two inertial orbits to have a closed relative orbit since their energies are equal. The ROE constraint is thus universally valid (no linearization).

Because of the coupling between semi major axis and orbital period, small uncertainties in the initial position and velocity result in a corresponding drift error and thus in a growing along-track error [11]. Long-term predictions of the relative motion between *Servicer* and *Client* are therefore sensitive to both orbit determination errors and maneuver execution errors. In order to minimize the collision risk of the two s/c in the presence of along-track position uncertainties, they must be properly separated in RN directions. As expected from the results of section 2.2 and shown in [6] this can be achieved by a (anti-)parallel alignment of the $\delta\underline{e}$ and $\delta\underline{i}$ vectors ($(\varphi - \theta) \in \{0, \pi\}$) . In this case RN separations never vanish at the same time and provide a minimum *safe* separation between the s/c at all times. This principle is termed *E/I separation*.

Perturbations of the motion such as J_2 and atmospheric drag effects can be easily incorporated through the convenient orbital elements description. The only perturbation which affect the E/I separation is the earth oblateness [11]. It turned out that choosing $\delta i_x = 0$ avoids a secular motion of $\delta\lambda$ and $\delta\underline{i}$ due to J_2 and provides hence a more *stable* configuration. Therefore the passively *safe* and *stable* configuration given through $\delta\underline{\alpha}_{nom} = \begin{pmatrix} \delta a & \delta\lambda & 0 & \pm\|\delta e\| & 0 & \pm\|\delta i\| \end{pmatrix}^{\mathrm{T}}$ is adopted as nominal configuration in this work.

Finally, all six relative state variables (position and velocity) are fast varying variables, meaning that they vary throughout the orbit. Using ROE simplifies the relative orbit computation because even within a perturbed orbit , e.g. gravitational perturbations, ROE will only change slowly. Due to its curvilinear nature large rectilinear distances can be captured by small ROE variations. This property is exploited and illustrated by the use of GVE for the relative control as described in the next section.

3. GAUSS' VARIATIONAL EQUATIONS

The Gauss' variational equations derived in [7] describe in the RTN frame the alteration of Keplerian Orbital elements due to a disturbance acceleration $\underline{\gamma}_p$. If the perturbation acceleration is due to a control thrust, GVE show what effect such a control thrust would have on the keplerian orbital elements. Based on the general GVE description in [7] it is possible to derive the GVE in terms of the non-singular orbital elements vector $\underline{\alpha}$ and build the limit for $e \to 0$ for a circular orbit. As result we get

$$\frac{\mathrm{d}a}{\mathrm{d}t} = 2a\frac{\gamma_{\mathrm{T}}}{na} \tag{16a}$$
$$\frac{\mathrm{d}u}{\mathrm{d}t} = n - 2\frac{\gamma_{\mathrm{R}}}{na} - \frac{\sin u}{\tan i}\frac{\gamma_{\mathrm{N}}}{na} \tag{16b}$$
$$\frac{\mathrm{d}e_x}{\mathrm{d}t} = 2\cos u\frac{\gamma_{\mathrm{T}}}{na} + \sin u\frac{\gamma_{\mathrm{R}}}{na} \tag{16c}$$
$$\frac{\mathrm{d}e_y}{\mathrm{d}t} = 2\sin u\frac{\gamma_{\mathrm{T}}}{na} - \cos u\frac{\gamma_{\mathrm{R}}}{na} \tag{16d}$$
$$\frac{\mathrm{d}i}{\mathrm{d}t} = \cos u\frac{\gamma_{\mathrm{N}}}{na} \tag{16e}$$
$$\frac{\mathrm{d}\Omega}{\mathrm{d}t} = \frac{\sin u}{\sin i}\frac{\gamma_{\mathrm{N}}}{na} \tag{16f}$$

Given an impulsive acceleration $\underline{\gamma}_p$ at a generic time t_0, the integration of the system of equations (16) over the impulse provides the relation between the maneuver $\Delta\underline{v}_{\mathrm{M}}$ and the subsequent change in orbital elements $\Delta\underline{\alpha}$ where $\Delta\underline{v}_{\mathrm{M}} = \int_{t_{\mathrm{M}}^-}^{t_{\mathrm{M}}^+} \underline{\gamma}_p \mathrm{d}t$ and $(\cdot_{\mathrm{M}})$ denotes the maneuver execution time

For proximity operations, these equations can be generalized from describing the motion of single spacecraft to the description of the relative motion of two spacecraft. This approach is the most natural way to control relative orbital elements and have the main advantage that it allows us to translate the aforementioned advantages of the ROE parametrization into maneuver planning.

3.1. Impulsive Thrust

We can extend the result above for relative motion. Let τ_f the dimensionless final time immediately after the maneuver and τ_i the dimensionless initial time. The alteration in relative orbital elements can be expressed a s a function of the absolute orbital elements at different dimensionless times

$$\Delta\delta\underline{\alpha} = f(\underline{\alpha_2}(\tau_{\mathrm{M}}^+), \underline{\alpha_2}(\tau_{\mathrm{M}}^-), \underline{\alpha_1}(\tau_{\mathrm{M}}^+), \underline{\alpha_1}(\tau_{\mathrm{M}}^-)) \tag{17a}$$

We obtain the direct relation between velocity increments in the RTN frame and the consequent change of ROE:

$$\Delta\delta\underline{\alpha}(u) = \frac{1}{n_2 a_2}\underline{\underline{G}}(u, u_{\mathrm{M}})\Delta\underline{v}_{\mathrm{M}} \quad , \quad \text{with}$$

$$\underline{\underline{G}}(u_{\mathrm{M}}) = \begin{bmatrix} 0 & 2 & 0 \\ -2 & -3(u - u_{\mathrm{M}}) & 0 \\ \sin u_{\mathrm{M}} & 2\cos u_{\mathrm{M}} & 0 \\ -\cos u_{\mathrm{M}} & 2\sin u_{\mathrm{M}} & 0 \\ 0 & 0 & \cos u_{\mathrm{M}} \\ 0 & 0 & \sin u_{\mathrm{M}} \end{bmatrix} . \tag{18}$$

$\Delta\delta\underline{\alpha}$ denotes the alteration of the ROE, $(\cdot_{\mathrm{M}})$ the maneuver execution time and $\Delta\underline{v}_{\mathrm{M}}$. It is possible to summarize the factor $1/n_2 a_2$ and $\Delta\underline{v}_{\mathrm{M}}$ to obtain the dimensionless velocity increment $\Delta\underline{\rho}'_{\mathrm{M}}$. Taking into account the evolution of the ROE described in (12) we deduce that the alteration of $\delta\lambda$ evolves after the maneuver linearly according to the following law

$$\Delta\delta\lambda = \delta\lambda_{\mathrm{M}} - 3(u - u_{\mathrm{M}}) \tag{19}$$

This result has been already incorporated in equation (18), so that $\underline{\underline{G}}(u_{\mathrm{M}}, u_{\mathrm{M}})$ decribes the *instantaneous* change in ROE while $\underline{\underline{G}}(u, u_{\mathrm{M}})$ takes into account the linear evolution of $\delta\lambda$.

3.2. Relation to The State Transition Matrix

It is worth noting that the inverse state transition matrix $\underline{\underline{\Phi}}^{-1}(u, u_0)$ in equation (15) and the variation matrix $\underline{\underline{G}}(u, u_{\mathrm{M}})$ in equation (18) are closely connected. We rewrite the mapping rule for convenience:

$$\Delta\delta\underline{\alpha}(u) = \underline{\underline{G}}(u, u_0)\Delta\underline{\rho}'_0 \tag{20a}$$
$$\delta\underline{\alpha}(u_0) = \underline{\underline{\Phi}}^{-1}(u, u_0)\delta\underline{x}(u) \tag{20b}$$

If we set $\delta\underline{\rho} = 0$, implying that both spacecrafts have same position but different velocities in the inverted linear motion model of equation (20b), we obtain the effect of an instantaneous velocity increment on the ROE vector [11]. Let $\underline{\underline{\Phi}}^{-1}$ in equations (15) be divided in four 3×3 blocks $\underline{\underline{\Phi}}_{ij}^{-1}(u, u_0)$, it follows

$$\delta\underline{\alpha}(u_0) = \left[\underline{\underline{\Phi}}_{12}^{-1}(u, u_0) \quad \underline{\underline{\Phi}}_{22}^{-1}(u, u_0)\right] \delta\underline{\rho}'(u) \tag{21}$$

Equations (21) and (18) are equivalent, the only difference between them is the opposite sign in the term $-3(u - u_{\mathrm{M}})$. This is due to the fact that the result is calculated for different mean argument of latitudes: u refers to after the maneuver while u_0 refers to the initial state.

The equations above assume impulsive maneuver which would require a propulsion source of infinite Thrust. In practice thrusts have always a finite duration which can be approximated as follow:

$$\Delta t_{\mathrm{M}} = m_2 \left\|\Delta \underline{v}_{\mathrm{M}}\right\| / F_{max} \ , \tag{22}$$

with F_{max} the available thrust level. Considering the execution as impulsive is a valid assumption for small maneuvers and thus adequate for maneuver planning. For large maneuvers the finite duration of the thrust has to be considered explicitly.

3.3. Finite-Duration Thrust

Depending on the amplitude of the maneuver, the mass of the s/c and the available thrust level, it is possible that the computed maneuver duration (22) is too large to be considered as impulsive. In this case, u_{M} cannot be considered constant during the maneuver anymore. Let $\underline{\gamma}_{\mathrm{M}}$ be the available level of acceleration in the RTN directions and $[t_1, \ t_2]$ the maneuver execution time interval. We integrated (18) and obtain

$$\Delta\delta\underline{\alpha} = \frac{1}{n_2^2 a_2}\underline{\underline{H}}(\tilde{u}_{\mathrm{M}}, \hat{u}_{\mathrm{M}})\underline{\gamma}_{\mathrm{M}} \ , \quad \text{with} \tag{23}$$

$$\mathbf{H}(\tilde{u}_{\mathrm{M}}, \hat{u}_{\mathrm{M}}) = \begin{bmatrix} 0 & 2\hat{u}_{\mathrm{M}} & 0 \\ -4\hat{u}_{\mathrm{M}} & -\frac{3}{2}\left(2\hat{u}_{\mathrm{M}}\right)^2 & 0 \\ 2\sin\tilde{u}_{\mathrm{M}}\sin\hat{u}_{\mathrm{M}} & 4\cos\tilde{u}_{\mathrm{M}}\sin\hat{u}_{\mathrm{M}} & 0 \\ -2\cos\tilde{u}_{\mathrm{M}}\sin\hat{u}_{\mathrm{M}} & 4\sin\tilde{u}_{\mathrm{M}}\sin\hat{u}_{\mathrm{M}} & 0 \\ 0 & 0 & 2\cos\tilde{u}_{\mathrm{M}}\sin\hat{u}_{\mathrm{M}} \\ 0 & 0 & 2\sin\tilde{u}_{\mathrm{M}}\sin\hat{u}_{\mathrm{M}} \end{bmatrix}, \tag{24}$$

$$\tilde{u}_{\mathrm{M}} = \frac{u(t_2) + u(t_1)}{2} \quad \text{and} \quad \hat{u}_{\mathrm{M}} = \frac{u(t_2) - u(t_1)}{2} \tag{25}$$

Note that $\hat{u}_{\mathrm{M}}$ is the halved dimensionless maneuver duration and $\tilde{u}_{\mathrm{M}}$ the mean argument of latitude at the middle point of the maneuver.

4. ASSESSMENT OF ORBITAL MANEUVERS

We assume that there are three different thrust directions: radial, along-track and normal. The fuel consumption FC due to a single impulse is proportional to the norm of the impulse vector. One impulse in normal direction is required to reconfigure the out-of-plane motion, while two in RT-direction are needed to reconfigure the in-plane motion. Based on the results of Vaddi etal.[9] and D'amico [11] we choose π as the optimal separation between two impulses.

Based on equation (18), one can deduce that radial maneuvers are safer than along-track ones since they do not affect the relative semi major axis and thus do not induce an evolving change (drift) in mean longitude. However, they are twice as expensive as along-track and are not able to achieve complete formation reconfiguration because the relative semi major axis can only be changed using along-track maneuvers. In this paper far range formation are considered, in which an approach via drift is desirable and thus exclusively along-track maneuvers are used for in-plane control. The insecurity is compensated through appropriate separation in RN-direction.

4.1. Impulsive Thrust Maneuvers

4.1.1. Out-of-Plane Maneuvers

The desired variation in the inclination vector can be obtained using maneuvers in normal direction. The influence of impulsive thrusts is given by equatio (18) where Δv_{N} is the normal impulsive thrust (scalar value) and u_{N} the location of the thrust. The non-trivial solution is given by a single thrust located at u_{N1} or $u_{\mathrm{N1}} + \pi$. Depending on the actual position on the orbit one can choose the closest solution to the actual position. However, operational constraints may suggest splitting the out-of-plane maneuver in two components located at u_{N1} and $u_{N1} + \pi$. This allows for example to correct maneuver execution errors. Let p be the thrust distribution coefficient, the double thrust solution is:

$$\begin{cases} \Delta v_{N1} = pna\|\Delta\delta\underline{i}\| & \text{at } u_{N1} = \arctan\left(\frac{\Delta\delta i_y}{\Delta\delta i_x}\right) \\ \Delta v_{N2} = (p-1)na\|\Delta\delta\underline{i}\| & \text{at } u_{N2} = u_{N1} + \pi, \ p \in [0,1] \end{cases} \tag{26}$$

4.1.2. Out-of-Plane Delta-V Budget

Single and double thrust impulsive maneuvers have the same delta-v budget:

$$FC = |\Delta v_{N1}| + |\Delta v_{N2}| = na\|\Delta\delta\underline{i}\| \tag{27}$$

4.1.3. In-Plane Maneuvers

The desired variation of the relative eccentricity vector $\delta\underline{e}$, relative semi major axis δa and relative mean longitude $\delta\lambda$ can be obtained using maneuvers in along-track and/or radial direction. The influence of impulsive thrusts is given by equation (18) where Δv_{R} and Δv_{T} are respectively the radial and along-track impulsive thrusts (algebraic values) , u_{R} and u_{T} the locations of the thrusts.

It is possible to control the relative eccentricity with a single thrust. The side effect is a persistent variation of the mean semi major axis and thus, an increasing change of the mean longitude. Beside operational constraints suggesting the splitting of maneuvers, a double-thrust solution can limit the instantaneous variation of semi major to between the thrusts. That means that, for $p = 0.5$, there is no change of the semi major axis but a change of the mean longitude at the end of the maneuver.

$$\begin{cases} \Delta v_{T1} = p\frac{1}{2}na\|\Delta\delta\underline{e}\| & \text{at } u_{T1} = \arctan\left(\frac{\Delta\delta e_y}{\Delta\delta e_x}\right) \\ \Delta v_{T2} = (p-1)\frac{1}{2}na\|\Delta\delta\underline{e}\| & \text{at } u_{T2} = u_{T1} + \pi \; p \in [0,1] \end{cases} \tag{28}$$

The pair of along-track maneuvers planned to settle the new $\delta\underline{e}$ vector change temporarily the relative semi major axis δa and thus cause a change of $\delta\lambda$. The caused drift between the maneuvers is $\Delta\delta\lambda = \pm\frac{3}{2}p\pi\|\Delta\delta\underline{e}\|$. Along-track maneuvers can be exploited to correct additionally the semi major axis[2]. One solution for the control of δa and $\delta\underline{e}$ is given by

$$\begin{cases} \Delta v_{T1} = \frac{1}{4}na\left(+\|\Delta\delta\underline{e}\| + \Delta\delta a\right) & \text{at } u_{T1} = \arctan\left(\frac{\Delta\delta e_y}{\Delta\delta e_x}\right) \\ \Delta v_{T2} = \frac{1}{4}na\left(-\|\Delta\delta\underline{e}\| + \Delta\delta a\right) & \text{at } u_{T2} = u_{T1} + \pi \end{cases} \tag{29}$$

The double thrust solution induces a non vanishing semi major axis difference that makes the spacecraft drift from each other. We have to take that into account in our control strategy and plan a second pair of maneuvers to stop the drift and acquire the desired mean longitude $\delta\lambda$ alteration (along-track separation). To stop (counteract) the variation of $\delta\lambda$ we aim a (slightly non) zero at the end of the second pair of maneuvers which make the spacecraft maintain the target separation (drift back). The caused drift between the maneuvers remains $\Delta\delta\lambda = \pm\frac{3}{4}\pi\|\Delta\delta\underline{e}\|$.

4.1.4. *In-Plane Delta-V Budget*

Since the choice of p does not influence the total fuel consumption we set $p = 0.5$ and obtain a homogeneous distribution.

$$FC = |\Delta v_{T1}| + |\Delta v_{T2}| = \frac{1}{2}na\|\Delta\delta\underline{e}\| \tag{30}$$

4.2. Finite-Duration Thrust Maneuvers

4.2.1. *Out-of-Plane Maneuvers*

The equation describing the influence of finite-duration thrusts on the out-of-plane motion is given by equation (23) where Δt_{N} is the duration of the thrust, γ_{N} is the normal thrust acceleration (scalar value) and u_{N} the location of the thrust. Analogously to the impulsive case, the solution for a homogeneous distribution ($p = 0.5$) is given by

$$\begin{cases} \Delta t_{N1} = \frac{2}{n}\arcsin\left(n^2 a\frac{\|\Delta\delta\underline{i}\|}{4|\gamma_{\mathrm{N}}|}\right) & \text{at } \tilde{u}_{N1} = \arctan\left(\frac{\Delta\delta i_y}{\Delta\delta i_x}\right) \\ \Delta t_{N2} = \frac{2}{n}\arcsin\left(n^2 a\frac{\|\Delta\delta\underline{i}\|}{4|\gamma_{\mathrm{N}}|}\right) & \text{at } \tilde{u}_{N2} = \tilde{u}_{N1} + \pi \end{cases} \tag{31}$$

where $\gamma_{\mathrm{N}} = \pm|\gamma_{\mathrm{N}}|$

4.2.2. *Out-of-Plane Delta-V Budget*

We consider the simple (and not limiting the generality) case of $p = 0.5$. The index refers to the number of maneuvers

$$\begin{cases} FC_1 = |\gamma_{\mathrm{N}}|\Delta t_{\mathrm{N}} \\ FC_2 = \sum_k |\gamma_{\mathrm{N}}|\Delta t_{Nk} = |\gamma_{\mathrm{N}}|\left(\Delta t_{\mathrm{N}1} + \Delta t_{\mathrm{N}1}\right) \end{cases} \tag{32}$$

Lemma 1. The splitting of the out-of-plane maneuvers reduces the propellant consumption

Proof. We define the function $h(x) = \arcsin\left(\frac{x}{2}\right) - \frac{1}{2}\arcsin(x)$. It can be shown that this function is monotonically decreasing for $x \in [-1, 1]$. It follows that

$$\begin{cases} h(0) = 0 \\ h \text{ monotone decreasing} \end{cases} \Rightarrow h(x) < 0 \forall x \in]0,1]$$

$$\Rightarrow \arcsin\left(\frac{x}{2}\right) < \frac{1}{2}\arcsin(x)$$

we set $x = n^2 a\frac{\|\Delta\delta\underline{i}\|}{2|\gamma_N|} \in]0,1]$

$$\Rightarrow \arcsin\left(n^2 a\frac{\|\Delta\delta\underline{i}\|}{4|\gamma_{\mathrm{N}}|}\right) < \frac{1}{2}\arcsin\left(n^2 a\frac{\|\Delta\delta\underline{i}\|}{2|\gamma_{\mathrm{N}}|}\right)$$

$$\Rightarrow \Delta t_{\mathrm{N}1} < \frac{1}{2}\Delta t_{\mathrm{N}1}$$

$\Rightarrow FC_2 < FC_1$ □

In a physical sense we can derive this result in the following way. The finite-duration thrust takes place along the arc length $\hat{u}_{\mathrm{M}}$The effectiveness of the maneuver is at maximum near the middle point $\tilde{u}_{\mathrm{M}}$. Splitting the maneuver provides two arcs separated by π and thus increases the effectiveness of the maneuver since the length of the portion in vicinity of $\tilde{u}_{\mathrm{M}}$ (two in our case) increases.

Lemma 2. The minimum of the (splitted) out-of-plane maneuver cost is given by a homogenous distribution ($p = 0.5$)

Proof. Let $h(p) = \arcsin(kp) + \arcsin(k(1-p))$, where k is a positive constant and p a real variable in$[0, 1]$.

$$\frac{\mathrm{d}}{\mathrm{d}p}h(p) = 0 \Leftrightarrow k[(1-(kp)^2)^{-1} - (1-k^2(1-p)^2)] = 0$$

$$\Leftrightarrow p^2 = (1-p)^2$$

$$\Leftrightarrow p = 0.5$$

Since $\frac{\mathrm{d}^2}{\mathrm{d}p^2}h(0.5) > 0$, we deuce that $h(p)$ has a global minimum at $p = 0.5$. $\square$

In a physical sense, we can derive this result in the following way. The length of the arc in vicinity of $\tilde{u}_{\mathrm{M}}$ is maximized for homogenous distribution and thus the effectiveness of the maneuver is maximized for $p = 0.5$

4.2.3. *In-Plane Maneuvers*

The equation describing the influence of finite-duration thrusts on the in-plane motion is given by equation (23) where $\Delta t_{\mathrm{R}}/\Delta t_{\mathrm{T}}$ is the duration of the thrust, $\gamma_{\mathrm{R}}/\gamma_{\mathrm{T}}$ is the radial/along-track thrust acceleration (algebraic value) and $u_{\mathrm{R}}/u_{\mathrm{T}}$ the location of the thrust. Analog to the impulsive case, the solution for a homogeneous distribution (p=0.5) is given by

$$\begin{cases} \Delta t_{\mathrm{T1}} = \frac{2}{n}\arcsin\left(n^2 a \frac{\|\Delta\delta\vec{e}\|}{8\|\gamma_T\|}\frac{1}{\cos\left(\frac{1}{2}n\frac{an\Delta\delta a}{4\|\gamma_{\mathrm{T}}\|}\right)}\right) + \frac{an\Delta\delta a}{4\|\gamma_{\mathrm{T}}\|} \\ \Delta t_{\mathrm{T2}} = \frac{2}{n}\arcsin\left(n^2 a \frac{\|\Delta\delta\vec{e}\|}{8\|\gamma_T\|}\frac{1}{\cos\left(\frac{1}{2}n\frac{an\Delta\delta a}{4\|\gamma_{\mathrm{T}}\|}\right)}\right) - \frac{an\Delta\delta a}{4\|\gamma_{\mathrm{T}}\|} \end{cases} \tag{33}$$

respectively at $\tilde{u}_{\mathrm{T1}} = \arctan\left(\frac{\Delta\delta e_y}{\Delta\delta e_x}\right), \tilde{u}_{\mathrm{T2}} = \tilde{u}_{T1} + \pi$ with $\gamma_{\mathrm{T}} = \pm\|\gamma_{\mathrm{T}}\|$

4.2.4. *In-Plane Delta-V Budget*

$$\begin{cases} FC_1 = |\gamma_{\mathrm{T}}|\Delta t_{\mathrm{T}} \\ FC_2 = \sum_k |\gamma_{\mathrm{T}}|\Delta_{\mathrm{T}k} = |\gamma_{\mathrm{T}}|\left(\Delta t_{\mathrm{T1}} + \Delta t_{\mathrm{T1}}\right) \end{cases} \tag{34}$$

5. CONTROL OF RELATIVE MOTION

5.1. Control Scheme

The control scheme in this paper is based on the following considerations

- Three different thrust directions (radial, along-track and normal) are available. This increases the fuel consumption in case skewed thrusts are needed but is still a valid assumption since maneuvers are typically constraint to certain directions.
- The reconfiguration of $\delta\underline{e}$ using two along track maneuvers is an optimal solution in that case [9, 11].
- The two along-track thrusts can be used to simultaneously reconfigure δe_x, δe_y and δa (and hence a non-vanishing variation of $\delta\lambda$). This is still an adequate sub-optimal solution for the in-plane reconfiguration since generally δa remains small.
- To stop a drift (i.e. set δa to zero) we need two pulses so that only δa is affected. Obviously, $\delta\lambda$ is also affected from the maneuver but has a constant value after the execution. δe_x and δe_y change only between the two maneuvers and finally take on their initial values at the end of the maneuvers.

The formation reconfiguration and formation keeping are performed using the concept illustrated in Fig. 4 which is valid for the general case of $\delta a \neq 0$ and for the finite-duration thrust case. The desired change of the relative semi major axis is split in $\Delta\delta a = \Delta\delta a_{\mathrm{I}} + \Delta\delta a_{\mathrm{II}}$. Two along-track maneuvers settle a change of the relative eccentricity vector $\Delta\delta\underline{e}$ and the intermediate change of the relative semi major axis $\Delta\delta a_{\mathrm{I}}$. Due to the new settled semi major axis $\delta\lambda$ will evolve with a constant rate until a second pair of along-track maneuvers provoke the second semi major axis change $\Delta\delta a_{\mathrm{II}}$. Commonly the second pair will stop the drift by setting δa to zero. $\Delta\delta a_{\mathrm{I}}$ has to be chosen in a way so that the total drift (inclusive between the maneuver pairs) corresponds to the desired change $\Delta\delta\lambda$. For the out-of-plane motion a single pulse split in two equivalent pulses will reconfigure $\delta\underline{i}$.

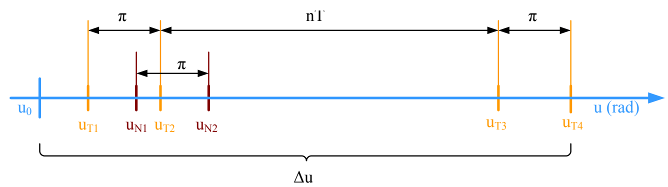

Fig. 4. Exemplary maneuver sequence for complete formation reconfiguration

5.1.1. *Impulsive Scheme*

Based on the results of the last section, we derived the 6 impulsive thrusts (IT) as follows:

$$\Delta v_{\mathrm{T1}} = \frac{1}{4}na\left(\Delta\delta a_I + \|\Delta\delta\underline{e}\|\right) \quad \text{at } u_{\mathrm{T1}} = \varphi \tag{35a}$$

$$\Delta v_{\mathrm{T2}} = \frac{1}{4}na\left(\Delta\delta a_I - \|\Delta\delta\underline{e}\|\right) \quad \text{at } u_{\mathrm{T2}} = u_{\mathrm{T1}} + \pi \tag{35b}$$

$$\Delta v_{\mathrm{T3}} = \frac{1}{4}na\Delta\delta a_{\mathrm{II}} \quad \text{at } u_{\mathrm{T3}} = u_{\mathrm{T2}} + nT \tag{35c}$$

$$\Delta v_{\mathrm{T4}} = \frac{1}{4}na\Delta\delta a_{\mathrm{II}} \quad \text{at } u_{\mathrm{T4}} = u_{\mathrm{T3}} + \pi \tag{35d}$$

$$\Delta v_{\mathrm{N1}} = +\frac{1}{2}na\|\Delta\delta\underline{i}\| \quad \text{at } u_{\mathrm{N1}} = \theta \tag{35e}$$

$$\Delta v_{\mathrm{N2}} = -\frac{1}{2}na\|\Delta\delta\underline{i}\| \quad \text{at } u_{\mathrm{N2}} = u_{\mathrm{N1}} + \pi \tag{35f}$$

The intermediate change of the relative semi major axis can be determined analytically ([15]):

$$\Delta\delta a_{\mathrm{I}} = \frac{-\frac{2\Delta\delta\lambda}{3} - \frac{\pi\|\Delta\delta\underline{e}\|}{2} - \delta a_0\left(u_{\mathrm{T1}} - u_0 + nT + 2\pi\right) - \frac{\Delta\delta a}{2}}{nT + \pi} \tag{36}$$

5.1.2. *Finite-Duration Scheme*

Based on equation (23), we extended the solution in equation (35) to the case of finite-duration thrusts (FDT)

$$\hat{u}_{\mathrm{T1}} = \arcsin\left(\frac{n^2 a\|\Delta\delta\underline{e}\|}{8|\gamma_T|\cos\left(\frac{n^2 a\Delta\delta a_{\mathrm{I}}}{8|\gamma_T|}\right)}\right) + \frac{an^2\Delta\delta a_{\mathrm{I}}}{8|\gamma_T|} \tag{37a}$$

$$\hat{u}_{\mathrm{T2}} = \arcsin\left(\frac{n^2 a\|\Delta\delta\underline{e}\|}{8|\gamma_T|\cos\left(\frac{n^2 a\Delta\delta a_{\mathrm{I}}}{8|\gamma_T|}\right)}\right) - \frac{an^2\Delta\delta a_{\mathrm{I}}}{8|\gamma_T|} \tag{37b}$$

$$\hat{u}_{\mathrm{T3}} = +\frac{an^2\Delta\delta a_{\mathrm{II}}}{8|\gamma_T|} \tag{37c}$$

$$\hat{u}_{\mathrm{T4}} = +\frac{an^2\Delta\delta a_{\mathrm{II}}}{8|\gamma_T|} \tag{37d}$$

$$\hat{u}_{\mathrm{N1}} = \frac{2}{n}\arcsin\left(n^2 a\frac{\|\Delta\delta\underline{i}\|}{4|\gamma_N|}\right) \tag{37e}$$

$$\hat{u}_{\mathrm{N1}} = \frac{2}{n}\arcsin\left(n^2 a\frac{\|\Delta\delta\underline{i}\|}{4|\gamma_N|}\right) \tag{37f}$$

Note that the middle point of each maneuver $\tilde{u}_{\mathrm{M}}$ matches exactly the pulse location u_{M} of the IT above. Furthermore $\Delta\delta a_{\mathrm{I}}$ involves solving a transcendental equation and can not be calculated analytically in case of finite-duration maneuvers. One possible approach is to approximate $\Delta\delta a_{\mathrm{I}}$ to the value computed via impulsive planning in equation (36) [16]. The transcendental equation can be approximated to a polynomial equation and solved via numerical iteration. First tests show that sufficiently accurate results are obtained after 3 to 6 iteration steps. This issue will not be treated in this paper.

5.2. Simulation

In this section the proposed control schemes are verified through a numerical integration of the nonlinear differential equations of motion using a Matlab-Simulink simulation environment. An assessment of the achievable performance via closed loop simulation is presented. The boundary conditions were defined assuming unperturbed motion and a *Servicer* s/c with a mass of 870 kg and a maximal thrust level of 0.4N. As described in section 2.4 a passively safe and stable configuration has been defined as $\delta\underline{\alpha}_{nom} = \begin{pmatrix}\delta a & \delta\lambda & 0 & \pm\|\delta e\| & 0 & \pm\|\delta i\|\end{pmatrix}^{\mathrm{T}}$. The initial and targeted final ROE used in the simulation are listed in Table 1.

Table 1. Initial and final configurations

	$a\delta a$	$a\delta\lambda$	$a\delta e_x$	δe_y	$a\delta i_x$	$a\delta i_y$
Initial(m)	29	-8000	0	0	0	0
Final (m)	0	-6000	0	-500	0	250

5.2.1. *Formation reconfiguration*

We examine an approach phase including a complete formation reconfiguration (FR) and keeping(FK) (same desired configuration) with a maneuver set interval Δu corresponding to $12\mathrm{h}$. It's assumed that this frequency corresponds to the radar measurement update. The implemented algorithm compares the measured configuration (initial) to the desired one (final) and computes a set of 6 maneuvers based on the finite-duration scheme. This step is repeated after 12h to compute a maneuver set for formation keeping in case the desired configuration has not been reached or did not remain stable.

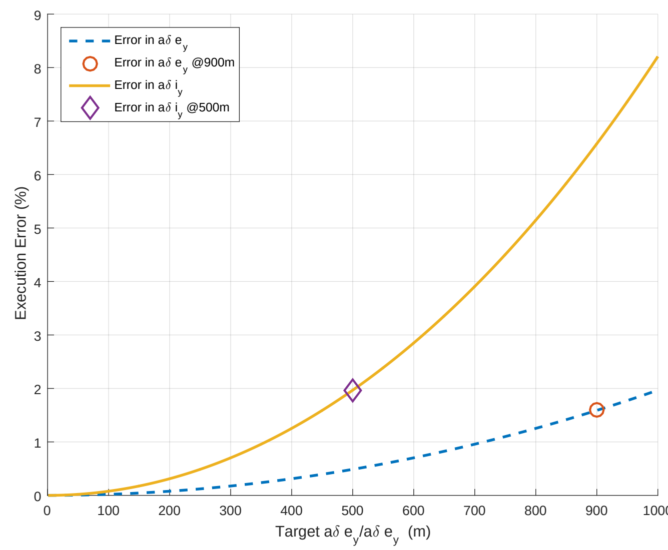

Fig. 5. Analytical assessment of formation error induced through impulsive planning.

Fig. 6 shows the temporal evolution of the individual ROE. The desired formation is achieved with high precision within the first 12h and remains stable so that no maneuvers are needed for the formation reconfiguration. The error is $9.8\mathrm{m}$ for $a\delta\lambda$ and remains under $1\mathrm{m}$ for the rest of the ROE. The temporal evolution of the elements coincides with the predicted behavior described in section 5.1 with the exception of small variations in $a\delta e_x$ and $a\delta i_x$ which are supposed to remain zero. This would be the case if the maneuvers are executed in an impulsive manner. Since maneuvers are executed along an arc centered at u_{M} a temporal change is induced which sums up to zero at the end of the maneuver.

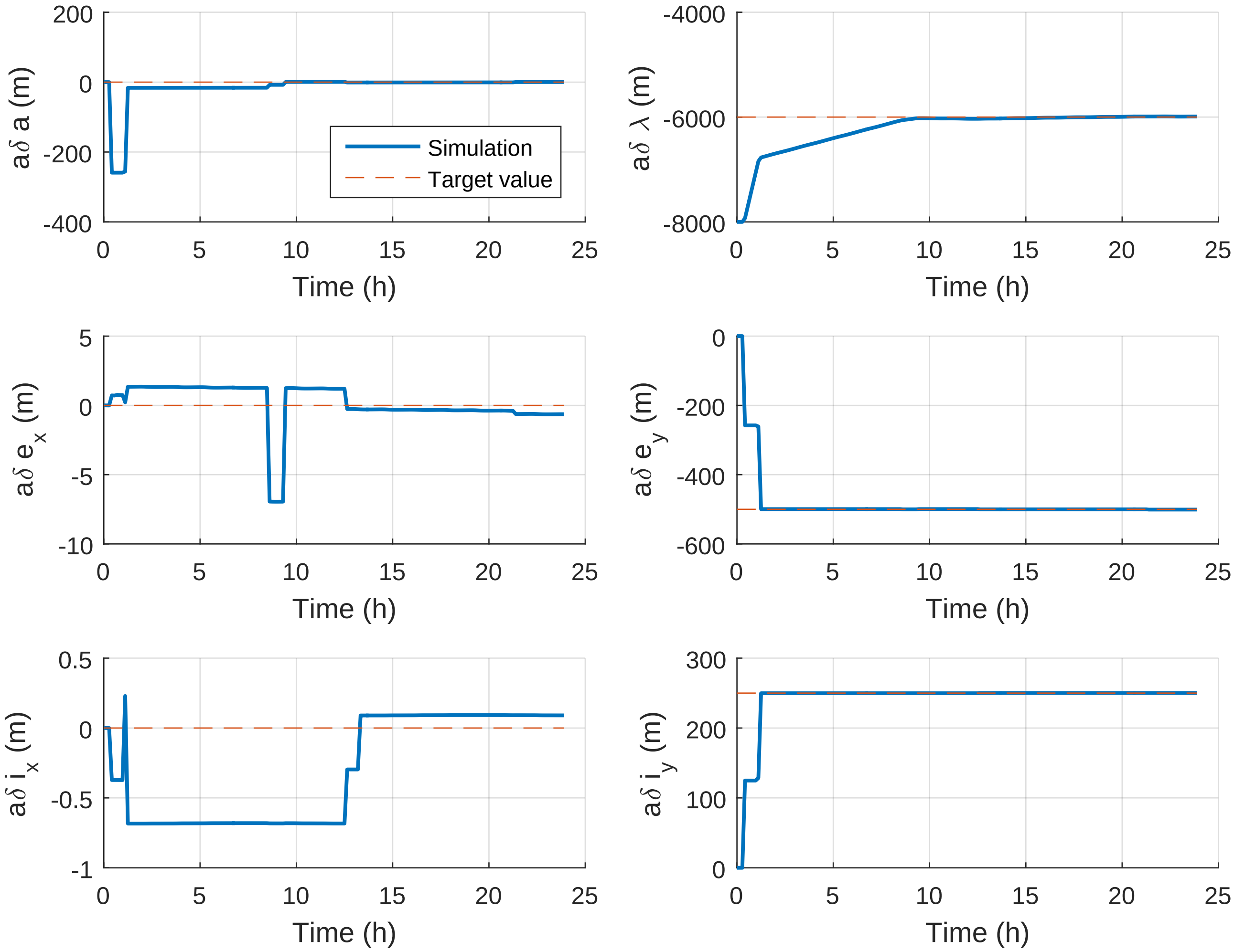

Fig. 6. Temporal evolution of the ROE during formation reconfiguration and formation keeping maneuvers

Further small discrepancies are explained as linearization errors.

5.2.2. Integrated GVE as Error Assessment Tool

It is possible to use the integrated GVE as precise (opposed to the standard GVE) analytical tool to propagate the effect of thrust maneuvers on ROE. We approximate the duration of maneuvers Δt_{M} For IT using (22). Inserting this Δt_{M} in(23) yields the induced alteration in ROE. This provides an *analytical* tool to estimate the error induced through impulsive planning. Depending on mission profile, this allows us to determine a threshold value (targeted alteration in ROE), for which impulsive planning is sufficient to achieve the required precision. Fig. 5 depicts the *analytical* error estimation for $a\delta e_y$ and $a\delta i_y$. The estimated errors ($1.6\,\%$ for $a\delta e_y$ and $2\,\%$ for $a\delta i_y$) coincide with simulation results.

6. REFERENCES

[1] H. Schaub and J.L. Junkins, *Analytical Mechanics of Space Systems, Second Edition*, AIAA Education series, virginia, 2009.

[2] J.S. Ardaens and S. D'Amico, "Spaceborne autonomous relative control system for dual satellite formations," *Journal of Guidance, Control, and Dynamics*, vol. 32, pp. 1859–1870, 2009.

[3] D. J. Kessler and B. G. Cour-Palais, "Collision frequency of artificial satellites: The creation of a debris belt," *Journal of Geophysical Research*, vol. 83, pp. 26372646, Januar 1978.

[4] J.-C. Liou, N. Johnson, and N. Hill, "Controlling the growth of future leo debris populations with active de-

bris removal," *Acta Astronautica*, vol. 66, pp. 648–653, 2010.

[5] C. Kebschul, J. Radtke, and H. Krag, "Deriving a priority list based on the environmental criticality," *International Astronautical Congress 2014, Toronto, Canada*, 2014.

[6] M.C. Eckstein, C.K. Rajasingh, and P. Blumer, "Colocation strategy and collision avoidancefor the geostationary satellites at 19 degrees west," *International Symposium on Space Flight Dynamics*, 1989.

[7] R. H. Battin, *An Antroduction to the Mathematics and Methods of Atsrodynamics, Revised Edition*, AIAA Education series, virginia, 1999.

[8] H. Schaub and K.T. Alfriend, "Impulsive feedback control to establish specific mean orbit elements of spacecraft formations," *Journal of Guidance, Control and Dynamics*, vol. 24, pp. 739–745, July 2001.

[9] S.S. Vaddi, K.T. Alfriend, S.R. Vadali, and P. Sengputa, "Formation establishment and reconfiguration using impulsive control," *Journalof Guidance, Control and Dynamics*, vol. 28, pp. 262–268, March 2005.

[10] L.S. Breger and J. P. How, "Gve-based dynamics and control for formation flying spacecraft," *2nd International Symposium on Formation Flying Missions and Technologies*, September 2004.

[11] S. D'Amico, *Autonomous Formation Flying in Low Earth Orbit*, Ph.D. thesis, Technical University of Delft, March 2010.

[12] Kyle T. Alfriend, R. Vadali Srinivas, Pini Gurfil, Jonathan P. How, and Louis S. Breger, *Spacecraft Formation Flying: Dynamics, control and navigation*, Elsevier, Oxford, 2010.

[13] D. L. Richardson and J. W. Mitchell, "A third-order analytical solution for relative motion with a circular reference orbit," *AAS/AIAA Space Flight Mechanics Meeting*, vol. 51, January 2002.

[14] H. Schaub, Srinivas R. Vadali, J.L. Junkins, and K. T. Alfriend, "Spacecraft formation flying control using mean orbit elements," *AAS Journal of Astronautical Sciences*, 2000.

[15] M.K. Ben Larbi, "Control concept for deos far range formation flight," Diploma Thesis - University of Stuttgart, 2011.

[16] M.K. Ben Larbi and P. Bergner, "Concept for the control of relative orbital elements for non-impulsive thrust maneuver," *Embedded Guidance, Navigation and Control in Aerospace (EGNCA 2012), IFAC*, 2012.